Tian, Miao; Wan, Xingbang; Chen, Min; Taskinen, Pekka; Tiljander, Mia; Jokilaakso, Ari

Phase equilibria of FeO_x-SiO_2-Al_2O_3 slag system at 1200 °C and pO_2 of $10^{-8.6}$ atm

Published in:
Calphad: Computer Coupling of Phase Diagrams and Thermochemistry

DOI:
10.1016/j.calphad.2022.102502

Published: 01/12/2022

Document Version
Publisher's PDF, also known as Version of record

Please cite the original version:
Tian, M., Wan, X., Chen, M., Taskinen, P., Tiljander, M., & Jokilaakso, A. (2022). Phase equilibria of FeO_x-SiO_2-Al_2O_3 slag system at 1200 °C and pO_2 of $10^{-8.6}$ atm. *Calphad: Computer Coupling of Phase Diagrams and Thermochemistry*, *79*, Article 102502. https://doi.org/10.1016/j.calphad.2022.102502

CALPHAD: Computer Coupling of Phase Diagrams and Thermochemistry 79 (2022) 102502

Contents lists available at ScienceDirect

Calphad

journal homepage: www.elsevier.com/locate/calphad

Phase equilibria of FeO_x-SiO_2-Al_2O_3 slag system at 1200 °C and pO_2 of $10^{-8.6}$ atm

Miao Tian [a,b], Xingbang Wan [c], Min Chen [a], Pekka Taskinen [a], Mia Tiljander [d], Ari Jokilaakso [a,*]

[a] Department of Chemical and Metallurgical Engineering, School of Chemical Engineering, Aalto University, Kemistintie 1F, P.O. Box 16100, FI-00076, Aalto, Finland
[b] School of Metallurgy and Environment, Central South University, Changsha, 410083, China
[c] School of Energy Science and Engineering, Central South University, Changsha, 410083, China
[d] Geological Survey of Finland, Vuorimiehentie 2, 02150, Espoo, Finland

ARTICLE INFO

Keywords:
Equilibria
High-Al_2O_3 slag
Thermodynamic
Copper smelting

ABSTRACT

The increasing concentrations of metallic Al or Al_2O_3 in secondary copper resources like electronic wastes motivate research into the slag chemistry of high-Al_2O_3 iron silicate slags for optimizing the industrial smelting process. In this study, the effect of Al_2O_3 in slag on the phase equilibria of the FeO_x-SiO_2-Al_2O_3 slag system was experimentally investigated at 1200 °C and pO_2 of $10^{-8.6}$ atm. The high-temperature experiments were undertaken in silica and spinel crucibles in a controlled CO–CO_2 gas atmosphere, followed by rapid quenching and Electron Probe Microanalysis. The equilibrium compositions of liquid slags in the tridymite primary phase field, spinel primary phase field, and the three-phase invariant point were determined. The 1200 °C isothermal section was constructed for the FeO_x-SiO_2-Al_2O_3 system, and the results showed that Al_2O_3 can dissolve in the liquid slags to a maximum concentration of 17 wt%. The present experimental results were compared with the predictions by MTDATA and FactSage. It was found that the present experimentally determined liquid domain agreed well with the calculations by FactSage except the invariant point. However, the present isotherm in the spinel primary phase field of spinel displayed lower Al_2O_3 concentrations. The present results help regulating fluxing strategies of FeO_x-SiO_2-Al_2O_3 slags and optimizing smelting operations of recycling high-alumina concentration copper resources.

1. Introduction

Aluminum, iron, and copper represent the major components in the waste electrical and electronic equipment (WEEE) [1]. With the depletion of primary ores and increasing demand for metals, WEEE becomes an essential secondary copper resource due to its various valuable metals [2]. One possible method of recovering WEEE is the pyrometallurgical copper smelting process, in which aluminum and iron are easily oxidized to the smelting slags and copper can be selectively and efficiently extracted [3]. Compared with primary copper concentrates, WEEE brings a significant amount of alumina to the smelting process, producing high-alumina FeO_x–SiO_2-Al_2O_3 slags. The increasing Al_2O_3 concentration of smelting slags may affect the slag properties, such as emerging solid phases and metal loss in slags, which would significantly influence the industrial processes and metal recovery efficiency. Investigation on the effect of increasing Al_2O_3 concentration on the equilibrium relations of smelting slags is of great importance for efficient and stable smelting operation.

The slag properties of the FeO_x–SiO_2–Al_2O_3 system in equilibrium with metallic iron, metallic copper, and sulphidic copper matte have been investigated extensively (Table 1). Muan et al. [4,5] measured the phase equilibrium relations and the liquidus temperature of copper-free FeO–Fe_2O_3–SiO_2–Al_2O_3 slag system in a pO_2 range from $10^{-12.5}$ to 1 atm. Zhao et al. [6] determined the phase boundary lines in the iron-saturated Al_2O_3-“FeO”-SiO_2 system at Al_2O_3 concentrations from 0 to 6 wt%. It was found that the Al_2O_3 addition led to an expansion of the fayalite primary phase field towards the region with lower iron oxide concentrations and resulted in a decrease of the liquidus temperature by approximately 3°C for each 1 wt% of Al_2O_3 added. Snow [7] reported the equilibrium phase relations between FeO–SiO_2–Al_2O_3 slag and metallic iron at 1400°C in nitrogen atmosphere.

In typical black copper smelting conditions [8], equilibrium

---

* Corresponding author.

E-mail addresses: miaotian2016@126.com (M. Tian), xingbangwan@126.com (X. Wan), min.chen@aalto.fi (M. Chen), pekka.taskinen@aalto.fi (P. Taskinen), mia.tiljander@gtk.fi (M. Tiljander), ari.jokilaakso@aalto.fi (A. Jokilaakso).

https://doi.org/10.1016/j.calphad.2022.102502
Received 8 July 2022; Received in revised form 6 November 2022; Accepted 8 November 2022

compositions of high-alumina FeO_x–SiO_2–Al_2O_3 slags and metallic copper were examined when investigating the distribution behavior of trace elements. Reddy et al. [9,10] studied the distributions of copper and nickel between copper-nickel alloys and Al_2O_3-saturated iron silicate slags at 1200–1300°C and pO_2 of 10^{-10} to 10^{-8} atm. Nagamori et al. [11,12] reported the distributions of trace elements between metallic copper and FeO–Fe_2O_3–SiO_2–Al_2O_3 slags with Al_2O_3 concentrations of 4–10 wt% at 1200–1300°C and pO_2 of 10^{-11} to 10^{-6} atm. Derin and Yüsel [13] studied the solubility of cobalt in Al_2O_3-saturated iron silicate slags in equilibrium with cobalt-copper-iron alloys at 1400°C and pO_2 of $10^{-7.95}$ to $10^{-6.3}$ atm. Klemettinen et al. [14] investigated the equilibrium phase relations and copper distributions between metallic copper alloy and alumina-spinel saturated iron silicate slags at 1300°C and $pO_2 = 10^{-10}$ - 10^{-5} atm. Equilibria within the copper and alumina-bearing iron silicate slags were examined in alumina or silica saturation by Avarmaa et al. [15,16] at 1300°C and $pO_2 = 10^{-10}$ - 10^{-8} atm, focusing on the distribution behaviors of Ga, In, Ge, and Sn.

Concerning the copper matte smelting process, the slag chemistry of the FeO_x-SiO_2-Al_2O_3 system has been researched at silica saturation and spinel saturation. Chen et al. [17,18] investigated the effect of Al_2O_3 on the equilibrium phase relations between matte and silica-saturated iron silicate slags at 1300°C and pSO_2 of 0.1 atm and 0.5 atm. Sukhomlinov et al. [19] studied trace elements distributions between copper matte and silica-saturated fayalite slags with 5 wt% Al_2O_3 at 1300°C and pSO_2 of 0.1 atm. At pSO_2 of 0.25 atm, Fallah-Mehrjardi et al. [20] measured the phase relations of silica-saturated fayalite slags with Al_2O_3 concentration of 3–10 wt% at 1200°C, and equilibria with 2–18 wt% Al_2O_3 at 1300°C were examined by Abdeyazdan et al. [21]. In the spinel primary phase field, the equilibria of matte and FeO_x-SiO_2-Al_2O_3 slags were researched in the synthesized spinel (Fe_3O_4) crucibles at 1250°C and pSO_2 of 0.25 atm by Chen et al. [22].

In the previous studies, the phase relations for the FeO_x–SiO_2-Al_2O_3 ternary system were mainly conducted at silica saturation with a low Fe/SiO_2 ratio and Al_2O_3 concentration. However, with the increasing use of secondary copper resources in the industry, high-Al_2O_3 iron silicate slags under silica saturation [23] and spinel saturation [24] were produced. The fundamental thermodynamic phase equilibrium and slag chemistry are essential for industrial practice. As can be seen in the publications compiled in Table 1, only limited studies have been published on the slag system at 1200°C in controlled atmospheres. This accelerated the need for establishing phase relations of the FeO_x–SiO_2-Al_2O_3 system with the equilibrium of liquid slags, silica, and spinel for a range of Al_2O_3 concentrations under controlled smelting conditions to enrich the thermodynamic data.

The objective of this study was to investigate the equilibrium phase relations of the FeO_x–SiO_2-Al_2O_3 slag system at 1200°C and pO_2 of $10^{-8.6}$ atm. Three sets of experiments were conducted for investigating the effects of Al_2O_3 on equilibrium phase relations between slag, tridymite, spinel, and gas of FeO_x–SiO_2-Al_2O_3 slags with an Al_2O_3 concentration range from 0 to 23 wt%. The present experimental results were compared with calculations by FactSage and MTDATA, which provides guidance for updating the thermodynamic databases. The present experimentally determined equilibrium phase relations and chemical compositions of phases are essential for adjusting fayalite-based slag compositions with a high-alumina concentration and optimizing secondary copper smelting operations of industrial interest.

2. Experimental

2.1. Materials

High purity oxide powders of Fe_2O_3 (99.995 wt%, Alfa Aesar), SiO_2 (99.99 wt%, Umicore, 0.2–0.7 mm), and Al_2O_3 (99.99 wt%, Sigma-Aldrich) were utilized to prepare the initial slag mixtures. The preparation of the slag mixtures started with mixing the required amounts of components (Table 2) thoroughly in an agate mortar for approximately 30 min, followed by placing them in a desiccator for later use. Each sample was weighed as 0.20 g, then pressed into a 5 mm diameter pellet. For the experiments in the tridymite saturated and the tridymite-spinel double saturated domain, the bowl-shaped fused silica crucibles (H × O.D. = 6 × 10 mm) were used to support the sample pellets. For the experiments in the spinel primary phase field, spinel crucibles were employed as substrates for the samples. To evaluate the availability of molybdenum (Mo) for supporting matte-free oxide slags at 1200 °C with low oxygen partial pressure, a duplicate series of experiments were carried out in Mo crucibles which were prepared by folding the high

Table 1

Equilibrium investigations of FeO_x-SiO_2-Al_2O_3 slags in the literature.

Investigators	Type of slag	Al_2O_3 concentration	Crucible	logpO_2/atm	Temperature/°C	Ref
FeO_x-SiO_2-Al_2O_3 slag						
Present study	SiO_2 saturated	0-23 wt%	SiO_2	−8.6	1200	–
	Spinel saturated		Fe_3O_4			–
	SiO_2-spinel saturated		SiO_2			–
Muan et al.	FeO_x-SiO_2-Al_2O_3	4-34 wt%	Pt	−12.5~ 0	1050–1529	[4]
Muan et al.	FeO_x-SiO_2-Al_2O_3	4-37 wt%	Pt	−0.67(air)	1340–1684	[5]
Copper matte- FeO_x-SiO_2-Al_2O_3 slag						
Fallah-Mehrjardi et al.	SiO_2 saturated	3-10 wt%	SiO_2	$pSO_2 = 0.25$ atm	1200	[20]
Sineva et al.	Spinel saturated	2-8 wt%	Fe_3O_4	$pSO_2 = 0.25$ atm	1200	[25]
Abdeyazdan et al.	SiO_2 saturated	2-18 wt%	SiO_2	$pSO_2 = 0.25$ atm	1300	[21]
Chen et al.	SiO_2 saturated	8 wt%	SiO_2	$pSO_2 = 0.1$ atm	1300	[17]
Chen et al.	SiO_2 saturated	7-9 wt%	SiO_2	$pSO_2 = 0.5$ atm	1300	[18]
Chen et al.	Spinel saturated	2-4 wt%	Fe_3O_4	$pSO_2 = 0.25$ atm	1250	[22]
Sukhomlinov et al.	SiO_2 saturated	5 wt%	SiO_2	$pSO_2 = 0.1$ atm	1300	[19]
Copper alloy- FeO_x-SiO_2-Al_2O_3 slag						
Klemettinen et al.	Al_2O_3-spinel saturated	17 wt%	Al_2O_3	−10~ −5	1300	[14]
Avarmaa et al.	Al_2O_3-spinel saturated	20 wt%	Al_2O_3	−10~ −5	1300	[15]
Avarmaa et al.	SiO_2 saturated	10 wt%	SiO_2	−10~ −5	1300	[16]
Nagamori et al.	Se/Te/Sn distribution	4-10 wt%	Al_2O_3	−11~ −6	1200,1300	[11]
Reddy et al.	Al_2O_3 saturated	0-16 wt%	Al_2O_3	−10~ −8	1200–1300	[9]
Derin et al.	Al_2O_3 saturated	10 wt%	Al_2O_3	−7.95~ −6.3	1400	[13]
Copper matte- Metallic copper -FeO_x-SiO_2-Al_2O_3 slag						
Shimpo et al.	SiO_2 saturated	8 wt%	SiO_2	−13~ −8	1200	[26]
Metallic iron -slag						
Zhao et al.	SiO_2 saturated	0-6 wt%	Pt, Fe	Nitrogen	1140–1190	[6]
Snow et al.	Liquidus surface	8-69 wt%	Fe	Nitrogen	900–1380	[7]

Table 2
Equilibrium phase compositions of FeO_x-SiO_2-Al_2O_3 slags at 1200 °C and pO_2 of $10^{-8.6}$ atm (EPMA, wt%).

Sample No	Initial compositions/wt%			Crucible	Phase	Equilibrium phase compositions/wt%-normalized				Original total (Mo)
	Al_2O_3	SiO_2	Fe_2O_3			Al_2O_3	SiO_2	"FeO"	Fe/SiO_2	
Liquid - Tridymite										
F1	0	40	60	SiO_2	Liquid	–	33.99 ± 0.13	66.01 ± 0.13	1.51 ± 0.01	97.62
					Tridymite	–	99.54 ± 0.20	0.46 ± 0.20		99.40
F13	0	36	64	SiO_2	Liquid	–	33.89 ± 0.11	66.11 ± 0.11	1.52 ± 0.01	98.62
					Tridymite	–	99.30 ± 0.17	0.70 ± 0.17		100.21
F2	5	45	50	SiO_2	Liquid	7.13 ± 0.06	38.51 ± 0.03	54.36 ± 0.07	1.10 ± 0.00	99.26
					Tridymite	0.03 ± 0.01	99.14 ± 0.19	0.83 ± 0.18		97.42
F3-1	8	48	44	SiO_2	Liquid	11.67 ± 0.12	41.37 ± 0.11	46.96 ± 0.12	0.88 ± 0.00	100.45
					Tridymite	0.06 ± 0.02	99.07 ± 0.14	0.88 ± 0.14		99.16
F3-2	8	48	44	Mo	Liquid	11.80 ± 0.12	39.96 ± 0.22	46.80 ± 0.22	0.91 ± 0.01	99.00 (1.44 ± 0.04)
					Tridymite	0.08 ± 0.03	98.95 ± 0.14	0.97 ± 0.11		99.99 (0.00 ± 0.01)
F4	10	43	47	SiO_2	Liquid	10.70 ± 0.05	39.85 ± 0.14	49.45 ± 0.14	0.97 ± 0.01	99.31
					Tridymite	0.03 ± 0.01	99.17 ± 0.06	0.79 ± 0.06		100.75
Liquid - Tridymite - Spinel										
F5-20 h	13	47	40	SiO_2	Liquid	17.28 ± 0.61	45.00 ± 0.62	37.72 ± 1.19	0.65 ± 0.03	99.16
					Tridymite	0.07 ± 0.05	99.28 ± 0.17	0.65 ± 0.15		100.30
					Spinel	51.68 ± 0.31	0.12 ± 0.00	48.20 ± 0.31		100.42
F5-40 h	13	47	40	SiO_2	Liquid	16.78 ± 0.13	44.30 ± 0.17	38.92 ± 0.27	0.68 ± 0.01	98.87
					Tridymite	0.20 ± 0.16	98.39 ± 0.98	1.41 ± 0.92		99.81
					Spinel	48.37 ± 0.20	0.20 ± 0.08	51.44 ± 0.19		100.25
F6	20	47	33	SiO_2	Liquid	17.38 ± 0.49	44.79 ± 0.36	37.83 ± 0.81	0.66 ± 0.02	97.76
					Tridymite	0.31 ± 0.10	97.76 ± 0.53	1.93 ± 0.58		99.62
					Spinel	48.53 ± 0.24	0.10 ± 0.06	51.37 ± 0.19		99.22
F7-20 h	23	43	34	SiO_2	Liquid	18.11 ± 0.52	44.81 ± 1.12	37.08 ± 1.62	0.64 ± 0.05	98.65
					Tridymite	0.13 ± 0.02	99.14 ± 0.05	0.73 ± 0.06		99.59
					Spinel	48.89 ± 1.29	0.11 ± 0.02	51.00 ± 1.28		100.61
F7-40 h	23	43	34	SiO_2	Liquid	18.88 ± 0.47	45.94 ± 0.30	35.18 ± 0.76	0.60 ± 0.02	99.24
					Tridymite	0.40 ± 0.14	97.56 ± 0.34	2.04 ± 0.29		100.86
					Spinel	51.02 ± 0.25	0.06 ± 0.04	48.92 ± 0.23		100.84
F8	20	40	40	SiO_2	Liquid	17.57 ± 0.55	44.19 ± 0.87	38.24 ± 1.42	0.67 ± 0.04	98.46
					Tridymite	0.36 ± 0.27	97.75 ± 1.11	1.89 ± 0.93		99.90
					Spinel	47.84 ± 0.45	0.14 ± 0.02	52.02 ± 0.45		99.93
F9	20	32	48	Mo	Liquid	15.46 ± 0.21	41.69 ± 0.20	40.97 ± 0.29	0.76 ± 0.01	97.75 (1.89 ± 0.04)
					Tridymite	0.10 ± 0.02	99.02 ± 0.13	0.87 ± 0.12		100.62 (0.01 ± 0.00)
					Spinel	49.29 ± 0.72	0.19 ± 0.21	50.34 ± 0.59		99.48 (0.19 ± 0.03)
Liquid - Spinel										
F10	12	26	62	Spinel	Liquid	8.48 ± 1.18	33.88 ± 0.22	57.63 ± 1.37	1.32 ± 0.04	99.38
					Spinel	20.31 ± 1.80	0.38 ± 0.05	79.32 ± 1.77		99.72
F11	10	28	62	Spinel	Liquid	6.56 ± 0.39	33.33 ± 0.27	60.12 ± 0.50	1.40 ± 0.02	99.31
					Spinel	11.90 ± 0.33	0.55 ± 0.02	87.55 ± 0.32		99.61
F12	8	22	70	Spinel	Liquid	6.65 ± 0.58	32.91 ± 0.12	60.44 ± 0.54	1.43 ± 0.01	99.58
					Spinel	10.96 ± 0.37	0.63 ± 0.07	88.41 ± 0.32		99.12
F14	0	20	80	Spinel	Liquid	–	29.51 ± 0.16	70.49 ± 0.16	1.86 ± 0.01	99.25
					Spinel	–	1.14 ± 0.10	98.86 ± 0.10		99.47
F15	0	10	90	Mo	Liquid	–	28.82 ± 0.12	71.18 ± 0.13	1.92 ± 0.01	98.17 (0.01 ± 0.01)
					Spinel	–	0.48 ± 0.04	87.14 ± 0.73		98.48 (12.38 ± 0.75)

purity Mo foil into a crucible shape.

2.2. Experimental procedures

The high-temperature isothermal equilibration experiments were conducted at 1200 °C with the corresponding primary phases as substrates, followed by rapid quenching in an ice-water mixture and the direct phase analysis. The experiments were carried out in a vertical alumina tube furnace (Nabertherm RHTV 120–150/18, L × O. D. = 1200 × 45 mm) equipped with $MoSi_2$ heating elements, as shown in Fig. 1. The furnace temperature was regulated with a Eurotherm 3216 PID controller with an overall temperature accuracy of ±3 °C. A calibrated *S*-type Pt/Pt–10%Rh thermal couple, placed next to the sample inside the working tube, was used to monitor the actual temperature of the sample.

The samples were introduced into the furnace from the bottom of the working tube and hung in the cold zone by a molybdenum (Mo) wire. The CO–CO_2 gas mixture was led into the furnace tube for around 15 min to flush the residual air and stabilize the oxygen partial pressure, after which the samples were lifted up to the hot zone of the furnace for equilibration. All samples were pre-melted at 1250 °C for 30 min, followed by equilibration at 1200 °C for the required time. After equilibration, the bottom end of the work tube was immersed in the ice-water mixture, and the rubber stopper that sealed the tube was removed. Pulling up the wire, the samples were dropped directly into the ice-water mixture for quenching, so that the high-temperature phase assembles can be retained at room temperature within seconds.

At 1200 °C, the oxygen partial pressure in the working tube was controlled at $10^{-8.6}$ atm by mixing CO (99.99 vol%, Woikoski Oy, Finland) and CO_2 (99.99 vol%, Woikoski Oy, Finland) according to the reaction Eq. (1) [27]. The required oxygen partial pressure and gases proportion could be calculated by Eq. (2), where ΔG ($J\cdot mol^{-1}$) is the

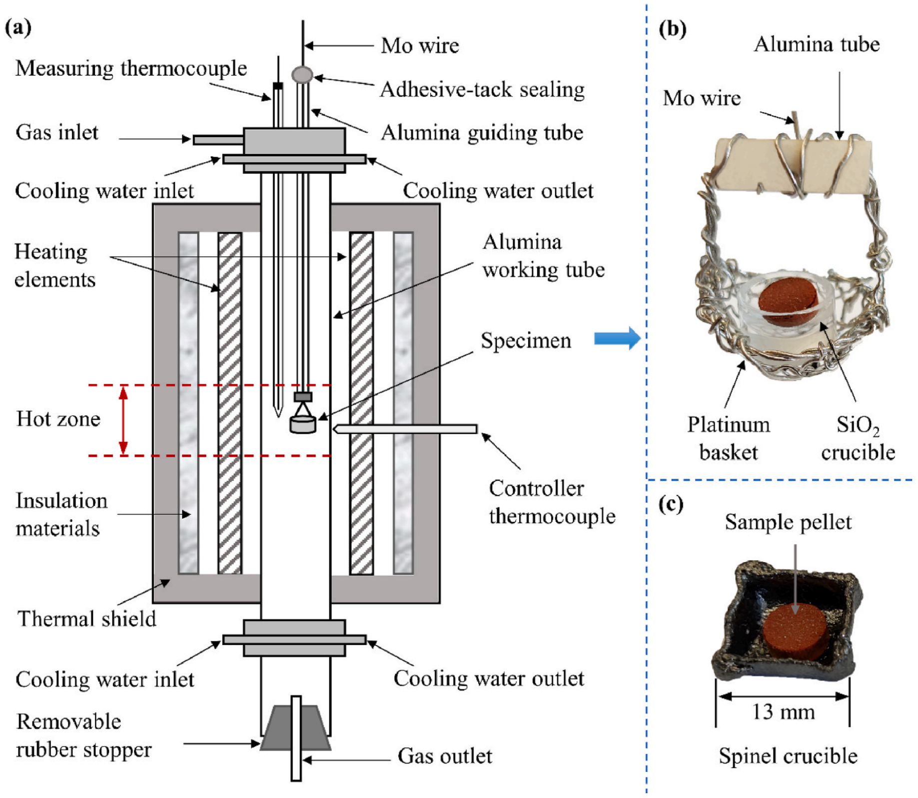

Fig. 1. Schematic of (a) the vertical furnace and the substrates used in the experiments: (b) SiO_2, (c) spinel.

standard Gibbs energy of reaction (1), R is the gas constant with a value of 8.314 (J mol^{-1} K^{-1}), P^{θ} is the standard atmospheric pressure 1 bar, pCO_2, pCO, and pO_2 are the partial pressures of CO_2, CO, and O_2. To generate the experimental condition of $pO_2 = 10^{-8.6}$ atm at 1200 °C, the gas flowrates of CO_2 and CO were regulated to 18 mL/min and 285 mL/min, respectively, using digital mass flow controllers (Aalborg, US) with a volumetric CO_2/CO ratio of 15.80. Argon gas (99.999 vol %, Woikoski Oy, Finland) was used for flushing the working tube prior to equilibration and for removing CO_2/CO gases after quenching.

$$2CO + O_2 = CO_2, \Delta G^{\theta}(kJ \bullet mol^{-1}) = -561.14 + 0.17T(K) \tag{1}$$

$$\lg(pO_2 / P^{\theta}) = 2\lg(pCO_2 / pCO) + 0.434\Delta G^{\theta} / RT \tag{2}$$

2.3. Analytical methods

The quenched samples were dried swiftly and mounted in epoxy resin (Epofix, Struers, Denmark). The sample surfaces were ground on waterproof silicon carbide abrasive papers and polished with metallographic polishing cloths using diamond sprays. The polished sections were carbon coated with a vacuum evaporator (JEOL IB-29510VET) carbon coater to ensure adequate electrical conductivity of the sample surfaces. The microstructures and phases compositions of all samples were pre-examined by a Scanning Electron Microscope (SEM, Tescan Mira3, Brno, Czech Republic) coupled with an UltraDry Silicon Drift Energy Dispersive X-ray Spectrometer (EDS, Thermo Fisher Scientific, Waltham, MA, USA) and NSS Microanalysis software, with an accelerating voltage of 15 kV and a beam current of 20 nA. At least six analysis points were randomly selected from each phase for statistical reliability. The Proza (Phi-Rho-Z) matrix correction procedure was used for processing the raw data [28]. The external standards utilized in EDS analyses were Al metal for Al Kα, hematite for Fe Kα, quartz for O Kα and Si Kα. The mineral and metal standards were supplied by Astimex (Toronto, Canada).

The elemental compositions of equilibrium samples were accurately analyzed with a CAMECA (SX100) electron microprobe analyzer (EPMA) using the wavelength dispersive spectrometry (WDS) technique. The accelerating voltage and beam current were 20 kV and 40 nA, respectively. A defocused beam diameter was set to 20 μm for the slag phases and to 5 μm for the tridymite and spinel phases. Natural and synthetic minerals were used as standards: pure Al_2O_3 for O Kα and Al Kα, quartz for Si Kα, hematite for Fe Kα, and metallic molybdenum for Mo Lα. The average elemental detection limits of EPMA were 1530 ppm for O, 159 ppm for Al, 176 ppm for Si, 176 ppm for Fe, and 345 ppm for Mo, respectively. Five to eight analysis points were randomly selected from the well-quenched area of each phase for statistical reliability. The analytical results have been corrected using the PAP on-line correction program [29].

2.4. Spinel crucible preparation

The spinel crucibles were prepared from high purity iron foil (thickness 0.25 mm, 99.5 wt%, Sigma Aldrich & Merck). The iron foil was folded into a box shape and the bottom was pressed into a bowl shape with a hemispherical stamping rod. The iron crucible was suspended in the hot zone of the vertical furnace by a platinum wire and oxidized for 2 h at 1250 °C and $pO_2 = 10^{-7}$ atm to generate spinel (Fe_3O_4). The oxidizing conditions for spinel crucible preparation were determined based on the Fe–O phase diagram predicted by FactSage 8.1 under different temperatures and oxygen partial pressures, as shown in Fig. 2(a). The oxygen partial pressure was controlled by a gas mixture of CO_2 (293.6 mL/min) and CO (6.4 mL/min) [30]. Finally, the synthesized crucible was moved to the cold zone of the furnace for 30 min and cooled to room temperature while maintaining the same gas mixture composition.

To identify the phase composition, one synthesized crucible was ground to powder and analyzed by X-Ray Diffraction (XRD, PANanalytical X'Pert Alpha 1, the Netherlands) with Cu Kα radiation under

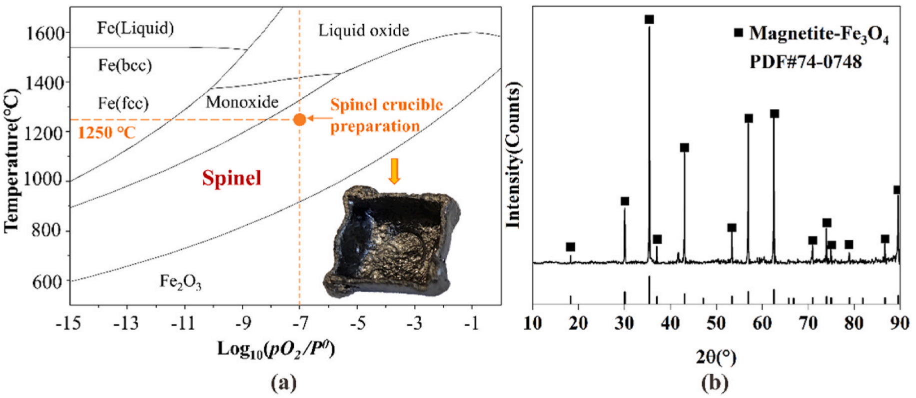

Fig. 2. (a) Stable regions of iron oxides as a function of temperature and oxygen partial pressure in the Fe–O phase diagram, calculated by FactSage 8.1, (b) XRD pattern of the synthesized spinel crucible.

45 kV, 40 mA. As shown in Fig. 2(b), the XRD pattern of the synthesized crucible indicates the metallic iron was fully oxidized to iron spinel (Fe_3O_4).

2.5. Thermodynamic calculation

In the present study, FactSage 8.1 and MTDATA were used to predict the isotherms of the FeO_x–SiO_2–Al_2O_3 slag system under fixed pO_2 of $10^{-8.6}$ atm at 1200 °C. In FactSage simulation [31], the databases of "FactPS" and "FToxide", and the solutions of "FToxid-SLAG", "FToxid-SPIN", "FToxid-MeO", "FToxid-Mull", "FToxid-CORU", and "FToxid-cPyrA" were selected to calculate the isotherms of the slag system using the "PhaseDiagram" module. In MTDATA simulation, a quasi-ternary liquidus contour FeO_x-SiO_2-Al_2O_3 slag was calculated using the Mtox database [32], including the solution phases of corundum, cordierite, liquid oxide, mullite, spinel, and tridymite.

3. Results

3.1. Equilibration time

A time series of experiment was conducted to determine the proper equilibration time for reaching homogenous liquid and solid compositions. The initial slag samples in the tridymite primary phase field (sample F5) and the tridymite-spinel double saturated domain (sample F7) with different Al_2O_3 concentrations were annealed at $pO_2 = 10^{-8.6}$ atm and 1200 °C for 5 h, 10 h, 20 h, and 40 h. The samples were premelted at 1250 °C for 30 min to promote the equilibration, after which temperature was lowered to 1200 °C for the duration of the experiments.

SEM-EDS was used to analyze the compositions and microstructures of the samples in the time series, as shown in Fig. 3. The required equilibration time was determined based on the stabilization of the compositions of the liquid phase. The liquid phase of the sample F5 and F7 was in contact with tridymite and spinel. The results show that the experimentally determined liquid compositions of sample F5 were in the tridymite-spinel double saturated domain, instead of in the computational tridymite primary phase field. Fig. 3(a) indicated that the liquid slag with an Al_2O_3 concentration of 13 wt% in the initial slag samples reached constant phase compositions within 10 h. However, in Fig. 3(b), the liquid slag with a 23 wt% Al_2O_3 concentration in the initial slags became homogenous within 20 h.

Therefore, all samples in the following experiments were annealed at the experimental conditions for at least 20 h to achieve uniform and constant phase compositions resembling the state of equilibrium.

3.2. Equilibrium phase relations of FeO_x-SiO_2-Al_2O_3 slags at 1200 °C and $pO_2 = 10^{-8.6}$ atm

Initial sample pellets with 0–23 wt% Al_2O_3 concentration were equilibrated at 1200 °C and $pO_2 = 10^{-8.6}$ atm to clarify the impact of Al_2O_3 concentration on the phase relations of fayalite-based slags. The typical microstructures of the quenched samples and the equilibrium phase compositions are shown in Fig. 4 and Table 2, respectively. As the EPMA is not sensitive to the oxidation degree of iron, the concentration of iron was recalculated to "FeO" for the ease of presentation. In the FeO_x-SiO_2-Al_2O_3 slag systems, two liquid-solid phase equilibria (i.e., liquid-tridymite and liquid-spinel), and one three-phase equilibrium

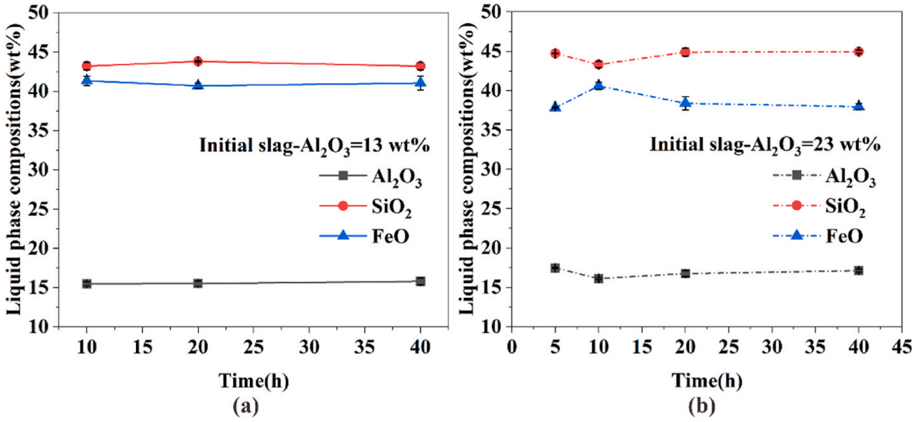

Fig. 3. The liquid phase compositions of the samples as a function of the equilibration time at 1200 °C and pO_2 of $10^{-8.6}$ atm, (a) sample F5 with 13 wt% Al_2O_3 and (b) sample F7 with 23 wt% Al_2O_3 in the initial slags (SEM-EDS data).

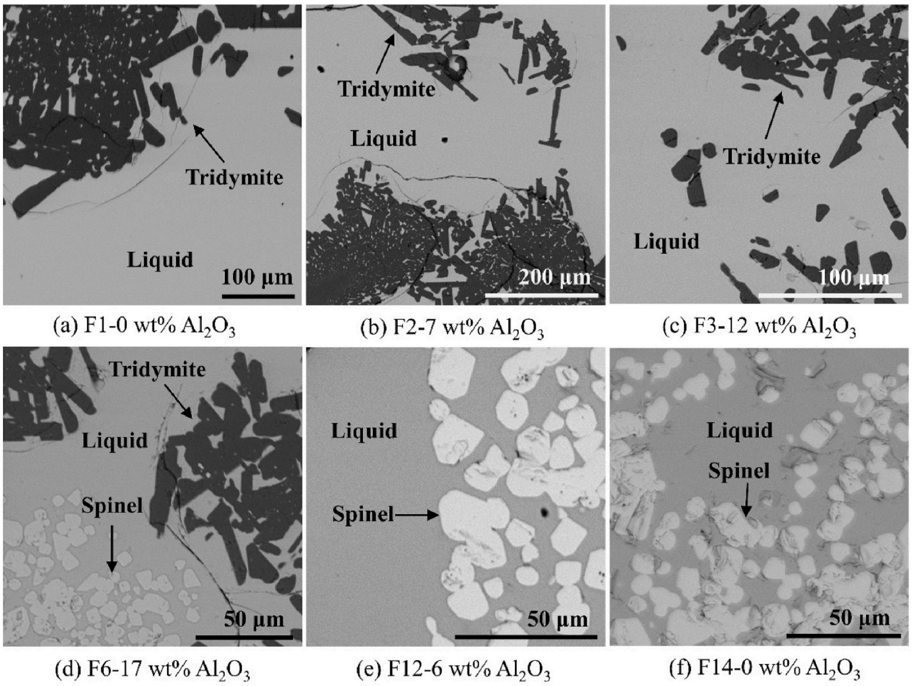

Fig. 4. Back scattered electron micrographs of the equilibrium phases of FeO_x-SiO_2-Al_2O_3 slags at 1200 °C and pO_2 of $10^{-8.6}$ atm. Tridymite- saturated domain, liquid-tridymite, (a) F1-0 wt% Al_2O_3, (b) F2-7 wt% Al_2O_3, (c) F3-12 wt% Al_2O_3.Tridymite-spinel saturated domain, liquid-tridymite-spinel, (d) F6-17 wt% Al_2O_3. Spinel saturated domain, liquid-spinel, (e) F12-6 wt% Al_2O_3, liquid-spinel, (f) F14-0 wt% Al_2O_3.

were observed for a wide range of Al_2O_3 concentrations.

When the Al_2O_3 concentration raised from 0 wt% to 12 wt%, a liquid-tridymite primary phase field was obtained in the high SiO_2 domain, as shown in Fig. 4(a)-4(c) in samples F1–F4. The black rod-like crystals were secondary tridymite resulting from the excessive dissolution of the silica crucible and the recrystallization of the excess silica as separate crystals. A liquid-spinel equilibrium was detected in the high “FeO” domain, as shown in samples F12 and F14 in Fig. 4(e) and (f).

A liquid-tridymite-spinel equilibrium was confirmed, when the Al_2O_3 concentration in slags was increased. As indicated in Fig. 4(d), three condensed phases of liquid, tridymite, and spinel were found in sample F6. The phase relations in the multicomponent equilibrium system can be determined by the Gibbs Phase Rule [33], and the number of phases are constrained by the degrees of freedom, as described by Eq. (3),

$$F = C - P + 2 \tag{3}$$

Where F is the degrees of freedom, C is the total number of independent components, P is the number of coexisting phases, and the number 2 refers to the environmental conditions of temperature and total pressure.

With a fixed temperature and total pressure of 1200 °C and 1 atm in this study, the degrees of freedom can be simplified as F= C–P. The FeO_x-SiO_2-Al_2O_3 slag has four independent components (C) and one of them is constrained (pO_2). The number of equilibrium phases (P) is 3 for the liquid-tridymite-spinel equilibria. Thus, the degrees of freedom (F) for the liquid-tridymite-spinel equilibria could be confirmed as F= C–P = 3 - 3 = 0, indicating that the liquid compositions for the liquid-tridymite-spinel three-phase equilibrium was constrained to a fixed point. This means the solubilities of SiO_2 and Al_2O_3 reached the maximum in the liquid slag phase, and the excess liquid oxides recrystallized as separate solid tridymite and spinel solid particles. The compositions of the coexisting solid oxides formed an invariant point in the present FeO_x-SiO_2-Al_2O_3 slag system.

As the liquid-tridymite-spinel coexisting equilibrium was observed in the samples F5–F8, the composition of the invariant point can be calculated using the average of samples F5–F8, which gave the composition of 17.7 (±0.7) wt% Al_2O_3 + 44.8 (±0.6) wt% SiO_2 + 37.5 (±1.3) wt% “FeO” for the liquid slag phase, and 49.4 (±1.6) wt% Al_2O_3 + 0.1 (±0.04) wt% SiO_2 + 50.5 (±1.5) wt% “FeO” for the coexisting solid spinel phase. The composition of tridymite was confirmed to be close to its stoichiometric value.

Furthermore, as Mo foil is much softer and more easily folded than iron foil, the use of Mo foil to support matte-free oxide slags was evaluated in repeated experiments, which aimed to simplify specific crucible preparation procedures. As listed in Table 2, for the equilibrium phases obtained using SiO_2 and spinel crucibles, the original totals of EPMA measurements before normalization were within 97.0–100.7 wt%. Some totals were slightly over 100 wt%, due to uncertainties in the EPMA analyzing technique.

As shown in Table 2, the Mo concentration in the liquid slag of the samples F3-2, F9, and F15 were 1.44 wt%, 1.89 wt%, and 0.01 wt%, respectively. In the tridymite phases of sample F3-2 and F9, the Mo concentration was below 0.01 wt%. In the spinel phases of sample F9 and F15, the dissolution of Mo was 0.19 wt% and 12.38 wt%, respectively. The results show that the equilibrium compositions of liquid slags were contaminated by quite high fractions of Mo. A large fraction of Mo dissolved in the spinel phase in the high “FeO” domain, while Mo was hardly at all distributed to the tridymite phase. Therefore, Mo foil is not suitable for holding the oxide slags at this condition because Mo dissolves in the liquid oxide and the spinel phase at high “FeO” concentrations.

3.3. Effect of Al_2O_3 on Fe/SiO_2 ratio of the liquid slag

According to the compositions given in Table 2, the increasing Al_2O_3 concentration led to decrease in the Fe/SiO_2 ratio, both in the primary phase fields of tridymite and spinel of the FeO_x-SiO_2-Al_2O_3 system. With increasing the Al_2O_3 concentration from 0 to 12 wt%, the Fe/SiO_2 ratio decreased from 1.52 to 0.88 in the tridymite-saturated slags, while it declined from 1.86 to 1.32 in the spinel saturated slags, presenting a higher Fe/SiO_2 ratio at the same Al_2O_3 concentration. The lowest Fe/

SiO_2 ratio in the liquid slag was 0.65 at the invariant point of tridymite-spinel double saturation.

The present experimental results showing the effect of Al_2O_3 concentration on the Fe/SiO_2 ratio were displayed in Fig. 5. Data from the literature were also plotted on the graph for comparison. Similarly to the current data, Shimpo et al. [26] reported that when compared with alumina-free system, the Fe/SiO_2 ratio got lower at 8 wt% Al_2O_3 in the slag in equilibrium with matte, metallic copper, and tridymite in the Cu–Fe–Si–Al–O system at 1200 °C and $pO_2 = 10^{-8}$ atm. Fallah-Mehrjardi et al. [20] found that the Fe/SiO_2 ratio in the liquid slag in equilibrium with matte and tridymite decreased significantly from 1.36 to 0.90 when Al_2O_3 concentration increased from 3 wt% to 10 wt% in the FeO_x--SiO_2-Al_2O_3 system at 1200 °C and $pSO_2 = 0.25$ atm, fitting well with the present work. Similar effect of Al_2O_3 addition on the Fe/SiO_2 ratio of spinel-saturated FeO_x-SiO_2-Al_2O_3 slag in equilibrium with matte at 1200 °C and pSO_2 of 0.25 atm was also observed by Sineva et al. [25].

4. Discussion

4.1. *Construction of the 1200 °C isotherm at pO_2 of $10^{-8.6}$ atm*

The 1200 °C isothermal section of the FeO_x-SiO_2-Al_2O_3 phase diagram at $pO_2 = 10^{-8.6}$ atm was constructed using the present experimental equilibrium phase compositions, as shown in Fig. 6. The primary phase fields of tridymite and spinel were determined at 1200 °C. The phase domain for liquid-tridymite-spinel three-phase equilibrium can be constructed by connecting the liquid point and the measured solid composition points of tridymite and spinel.

4.2. *Comparison between experimental and predicted results by MTDATA and FactSage*

The present experimental equilibrium phase relations of the FeO_x-SiO_2-Al_2O_3 system were compared with the predicted isothermal sections by MTDATA [18], with the same atmospheric constraint, as displayed in Fig. 7. The liquid point for the liquid-tridymite-spinel three-phase equilibrium obtained in this study was close to the predictions. The experimentally measured liquid slag domain was slightly narrower than the predictions by MTDATA. The present isotherm in the tridymite primary phase field agreed well with the simulations by MTDATA, while the present results in the spinel primary phase field exhibited a lower “FeO” but higher SiO_2 concentrations. Compared with MTDATA simulations, the spinel phase coexisted with liquid and tridymite in this study displayed a composition with a higher “FeO” but lower Al_2O_3 concentration.

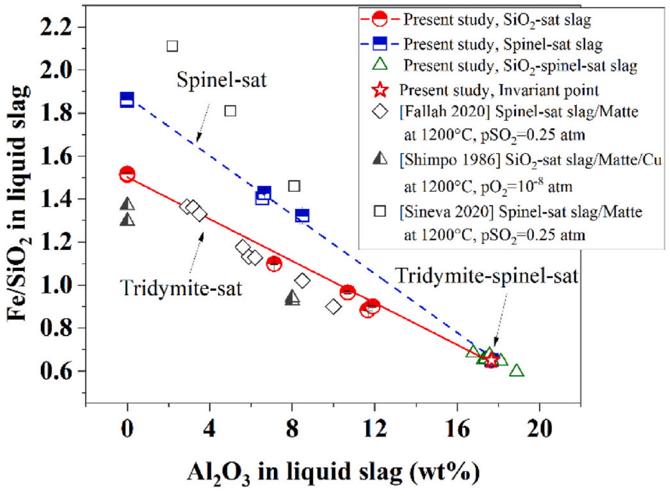

Fig. 5. The Fe/SiO_2 ratio of the liquid slag as a function of the Al_2O_3 concentration in the FeO_x-SiO_2-Al_2O_3 system in the present study and literature results [20,28,29].

As shown in Fig. 8, the isotherms experimentally determined in this study agreed well with the simulations by FactSage [34]. However, the composition of the spinel phase in equilibrium with the liquid slag and tridymite in current results had a higher “FeO” but lower Al_2O_3 concentration than the predictions by FactSage. It should be noticed that in the high Al_2O_3 concentration range, FactSage predicted the mullite primary phase field, and two three-phase equilibriums of liquid-mullite-spinel and liquid-tridymite-mullite, while the three-phase equilibrium of the liquid-tridymite-spinel domain was not obtained in the calculations. The presence of liquid-tridymite-spinel phase equilibrium in this study contradicts the existence of liquid-mullite two-phase equilibrium predicted by FactSage (Fig. 8).

It is evident that the simulations by FactSage and MTDATA deviate significantly in the mullite primary phase field and its stabilization temperature in this system. Mullite is a solid solution compound of alumina and silica that is stable above 1200 °C, with stoichiometries ranging from relatively silica-rich $3Al_2O_3{\cdot}2SiO_2$ to alumina-rich $2Al_2O_3{\cdot}SiO_2$ [35]. Muan et al. [5] found that the coexisting temperature for liquid-tridymite-spinel-mullite equilibrium in air was 1380 °C, below which the mullite disappeared and the liquid-tridymite-spinel equilibria formed. When pO_2 was reduced from 10^{-3} to $10^{-9.6}$ atm, the lowest stability temperature for the liquid-tridymite-spinel-mullite equilibrium decreased from 1230 °C to 1191 °C [4]. The liquidus temperature, thus, decreased when oxygen partial pressure was lowered.

In MTDATA, the enclosed liquidus surface diagram in temperature interval of 1100–1300 °C shows the mullite disappearing when temperature falls below about 1230–1240 °C, whereas FactSage predicts that the mullite primary phase field is stable above 1190–1200 °C. As a result, the stability temperature of mullite is too high in the FactSage database compared with data by Muan et al. [5] and this study. Furthermore, MTDATA was used to predict the 1300 °C isotherms of FeO_x-SiO_2-Al_2O_3 slags in equilibrium with matte [17] and copper alloy [14]. The calculated isotherms matched the FactSage predictions in Fig. 8, indicating mullite was stable at higher temperatures. However, because mullite formation was assumed to be slow, it may not have been visible in the experimental samples of the literature [36].

The predicted liquidus from MTDATA and FactSage were both provided for comparison in Fig. 9. The present experimentally determined liquid domain was consistent with the calculated results from MTDATA and FactSage, while the predictions by MTDATA extending the liquid compositions to a slightly higher “FeO” concentration area. As for the spinel in equilibrium with liquid and tridymite, the calculated values by MTDATA and FactSage exhibited a higher Al_2O_3 concentration. Small discrepancies between MTDATA and FactSage results can be attributed to differences in the selected databases and their thermodynamic data. However, the three-phase equilibrium calculated by FactSage was the mullite-spinel-liquid oxide system, whereas MTDATA predicted the invariant point as found in this study, between silica, spinel, and liquid oxide slag.

In Fig. 9, the experimental slag compositions observed by Fallah-Mehrjardi et al. [20] at 1200 °C and $pSO_2 = 0.25$ atm from the matte-slag-tridymite equilibrium system were also presented to show the impact of Al_2O_3 concentration. The reported slag compositions in the tridymite-saturated domain fitted well with the present study and Muan et al. [5], with Al_2O_3 concentrations ranging from 3 to 10 wt%.

4.3. *Spinel composition of the FeO_x-SiO_2-Al_2O_3 slags*

4.3.1. *“FeO”-Al_2O_3 binary system*

The spinel compositions of iron silicate slags in the present study and literature were plotted in the “FeO”-Al_2O_3 pseudo-binary plane in Fig. 10 and compared with the predictions to investigate the solubility of Al_2O_3 in the solid spinel phase at different conditions. All iron oxide in the spinel was recalculated to “FeO” for the ease of presentation.

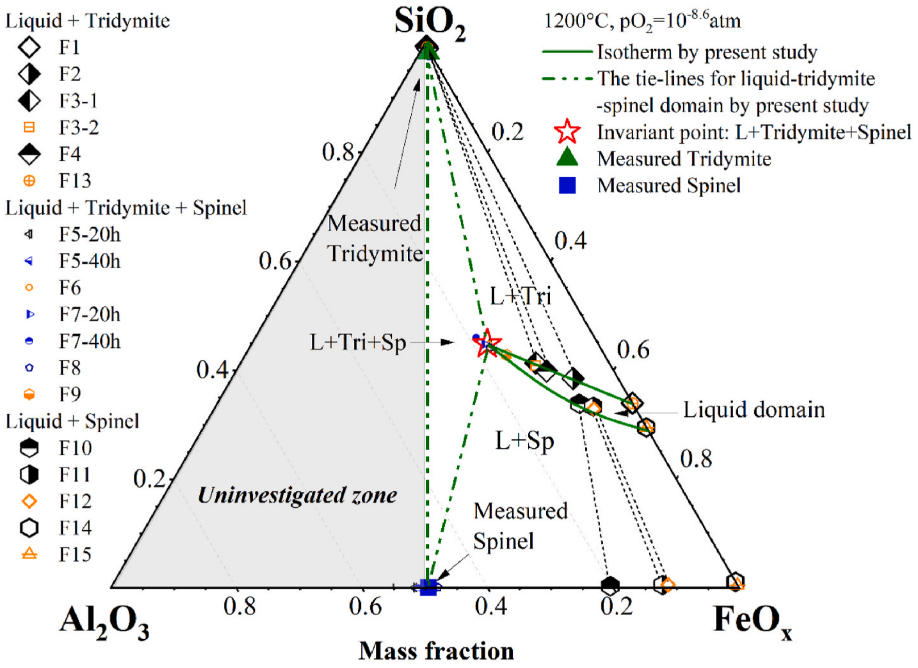

Fig. 6. The isotherm of the FeO_x-SiO_2-Al_2O_3 system of the present study at 1200 °C and pO_2 of $10^{-8.6}$ atm.

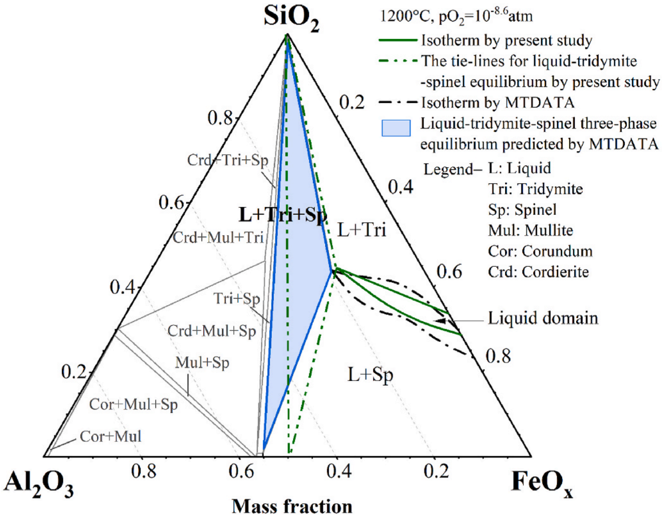

Fig. 7. A comparison of the isotherms from the present work and the predictions by MTDATA of FeO_x-SiO_2-Al_2O_3 system at 1200 °C and pO_2 of $10^{-8.6}$ atm.

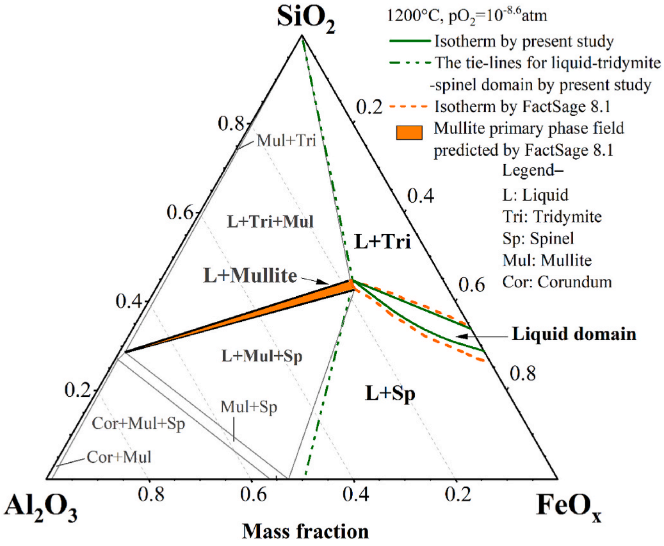

Fig. 8. A comparison of the isotherms from the present work and the simulations by FactSage of FeO_x-SiO_2-Al_2O_3 system at 1200 °C and pO_2 of $10^{-8.6}$ atm.

Klemettinen et al. [14] and Avarmaa et al. [15] observed the spinel composition of the iron-alumina spinel saturated iron silicate slag equilibrated with copper alloy in alumina crucibles at 1300 °C. They found that the spinel was almost pure $FeAl_2O_4$ at the reducing point ($pO_2 = 10^{-10}$ atm) with 59 wt% Al_2O_3, and turned to the iron-rich state with Al_2O_3 decreased to approximately 25 wt% at the oxidizing conditions when increasing the pO_2 to 10^{-5} atm. It was suggested that the spinel composition in the invariant point of the FeO_x-SiO_2-Al_2O_3 slags was highly dependent on the oxygen partial pressure [37], which agreed well with the spinel composition at the corundum-spinel phase boundary at 1300 °C predicted by FactSage.

However, for FeO_x-SiO_2-Al_2O_3 slags equilibrated with matte in the synthesized spinel (Fe_3O_4) crucibles, Chen et al. [22] found that the alumina concentration in the spinel increased from 6 wt% to 10 wt% with the oxygen partial pressure ranging from −7.9 to −7.5 at 1250 °C and pSO_2 of 0.25 atm. Sineva et al. [25] reported that the Al_2O_3 concentration in the recrystallized spinel increased along with the increasing solubility of Al_2O_3 in the liquid slag at 1200 °C and pSO_2 of 0.25 atm. The experimental data [22,28] suggested that when Al_2O_3 concentration in the liquid slag was lower than its maximum solubility, the spinel composition shifted from the iron-rich area (Fe_3O_4) of the spinel primary domain to the alumina-rich state with increased solubility of Al_2O_3 in the liquid slag.

In the present study, the experimentally determined spinel composition was pure Fe_3O_4 in the Al_2O_3-free iron silicate slags and exhibited a higher Al_2O_3 but lower “FeO” concentration when increasing the Al_2O_3 solubility in the coexisting liquid slag at the fixed oxygen partial pressure, similar to the data obtained by Sineva et al. [25]. In the current results, the spinel composition at the invariant point of tridymite-spinel double saturated slag was close to $FeAl_2O_4$, while presenting a slightly

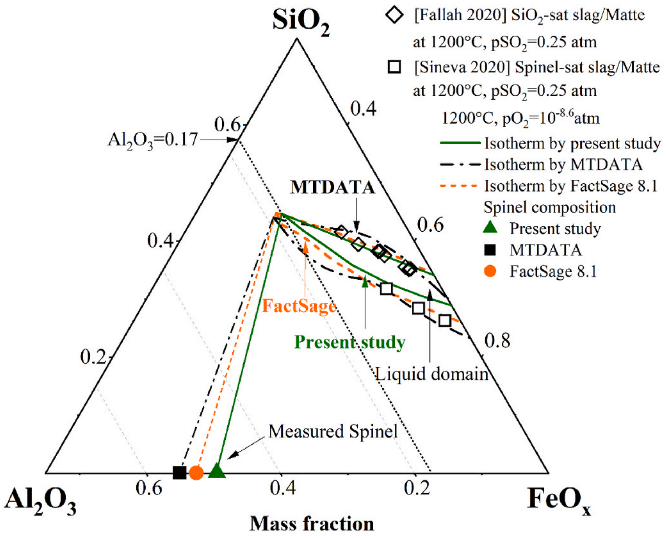

Fig. 9. A comparison of the present isotherms of FeO_x-SiO_2-Al_2O_3 system and data from the literature [20,25] at 1200 °C and pO_2 of $10^{-8.6}$ atm.

lower Al_2O_3 concentration compared with predictions by FactSage and MTDATA at 1200 °C. In the FactSage predictions, compared with the FeO_x-Al_2O_3 system, the spinel composition in the invariant point of the FeO_x-SiO_2-Al_2O_3 system displayed a higher “FeO” and lower Al_2O_3 concentration, due to the existence of the mullite phase in the FeO_x--SiO_2-Al_2O_3 system (Fig. 8).

4.3.2. *FeO–Fe_2O_3–Al_2O_3 ternary system*

The spinel composition in the FeO–Fe_2O_3–Al_2O_3 system was investigated by experimental observations [38,39] and thermodynamic assessments [40,41]. The spinel phase was a solid solution between Fe_3O_4 ($FeO{\cdot}Fe_2O_3$) and $FeAl_2O_4$ ($FeO{\cdot}Al_2O_3$) with some excess Fe_2O_3 or Al_2O_3. The Fe^{2+}/Fe^{3+} ratio in the spinel varies with the temperature and oxygen partial pressure [38]. Muan et al. [38] experimentally investigated the amount of FeO and Fe_2O_3 in the spinel of the FeO–Fe_2O_3–Al_2O_3 system by chemical analysis. Shishin et al. [40] simulated the spinel region of Fe_2O_3–Fe_3O_4–$FeAl_2O_4$ by thermodynamic model. Lindwall et al. [41] calculated the concentration of FeO and Fe_2O_3 in the spinel of the FeO–Fe_2O_3–Al_2O_3 system by optimizing model parameters.

In this study, the concentrations of Fe and O in the spinel phase were measured by EPMA. The oxidation states of iron could not be measured, as the EPMA was not sensitive to the valence of iron. Due to the negligible SiO_2 concentration in the spinel, the spinel composition would be close to the ternary FeO–Fe_2O_3–Al_2O_3 system [37]. As shown in Table 3, the mass fraction of FeO and Fe_2O_3 in the spinel phase could be calculated based on the elemental compositions measured by EPMA through the following equations,

$$m_{O-total} = m_{O-FeO} + m_{O-Fe_2O_3} + m_{O-Al_2O_3} \tag{4}$$

$$m_{Fe-total} = m_{Fe-FeO} + m_{Fe-Fe_2O_3} \tag{5}$$

where $m_{\text{o-total}}$ and $m_{\text{Fe-total}}$ represent the mass of O and Fe in the spinel measured by EPMA. The $m_{\text{o-i}}$ is the mass of O in the FeO, Fe_2O_3, and Al_2O_3 of the spinel. The $m_{\text{Fe-i}}$ is the mass of Fe in the FeO and Fe_2O_3 of the spinel.

The spinel compositions in the present study (Table 3) and the predictions by FactSage 8.1 were projected onto the FeO–Fe_2O_3–Al_2O_3 ternary system (Fig. 11) for comparison. In the FactSage predictions, the spinel composition shifted to the FeO higher concentration area and was close to the Fe_3O_4–$FeAl_2O_3$ join when the pO_2 decreased from 10^{-3} to $10^{-8.6}$ atm at 1200 °C. Compared with the predictions by FactSage, the experimentally determined spinel composition in this study displayed a higher FeO but a lower Fe_2O_3 concentration. When Al_2O_3 concentration in the spinel increased, the spinel in the present study occurred between the composition points of Fe_3O_4 and $FeAl_2O_3$, with some excess FeO. The ratio of Fe^{3+} to the total iron in the spinel-saturated fayalite slags [42] predicted by FactSage was below 0.2 at 1200 °C and pO_2 of $10^{-8.6}$ to $10^{-7.9}$ atm, which indicated the excess Fe^{2+} in the slags.

In Fig. 12, the 1500 °C and 1200 °C isotherms of the FeO–Fe_2O_3–Al_2O_3 ternary system were calculated by FactSage 8.1 and by Lindwall et al. [41], respectively. The calculated isotherms of the spinel primary phase field displayed a higher FeO but lower Fe_2O_3 concentration area when the temperature decreased. Atlas et al. [43] investigated the spinel composition by equilibrium experiments in a helium atmosphere at temperatures of 1000, 1250, and 1350 °C. It was founded that the width of the spinel primary phase field was temperature-dependent and was limited by the ability of the spinel structure to tolerate cation deficiencies at various temperatures. The spinel vertex of the Spinel-Corundum equilibria exhibited a lower FeO but a higher Al_2O_3 concentration with increasing temperature.

Roiter et al. [44] researched the range of oxygen partial pressure for preparing the spinel phase at 1500 °C. As shown in Fig. 12, they found that a definite oxygen partial pressure was necessary for maintaining the spinel phase. Oxygen partial pressure lower than the definite value would produce two-phase materials. Similar conclusions were obtained by the predicted isobars of pO_2 in the 1200°C isotherm of the

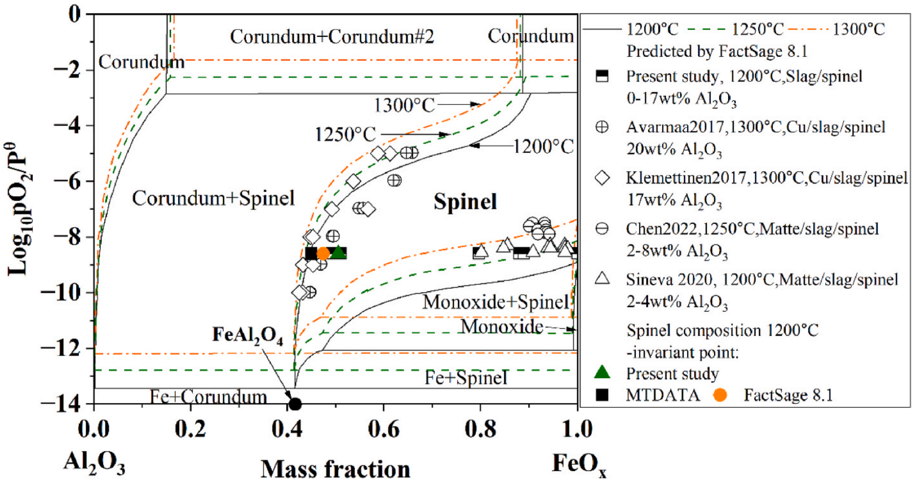

Fig. 10. Oxygen partial pressures and phase boundaries of the FeO_x-Al_2O_3 system calculated by FactSage 8.1, and the experimentally determined spinel composition of the present study and literature [14,15,22,25].

Table 3

Equilibrium composition of the spinel in the FeO_x-SiO_2-Al_2O_3 slags at 1200 °C and pO_2 of $10^{-8.6}$ atm (wt%).

Sample No	Elemental composition measured by EPMA				Original total	Normalized composition		
	O	Al	Si	Fe		Al_2O_3	FeO	Fe_2O_3
Invariant point	34.9 ± 0.7	26.0 ± 0.8	0.1 ± 0.0	39.0 ± 1.3	100.1	49.1	43.1	7.8
F10	29.93 ± 0.38	10.37 ± 0.93	0.17 ± 0.02	59.53 ± 1.28	99.72	19.63	42.05	38.33
F11	28.74 ± 0.22	6.01 ± 0.17	0.25 ± 0.01	65.00 ± 0.28	99.61	11.39	39.07	49.55
F12	28.34 ± 0.11	5.56 ± 0.20	0.28 ± 0.03	65.82 ± 0.16	99.12	10.52	42.08	47.39
F14	25.70 ± 0.30	–	0.51 ± 0.04	73.78 ± 0.32	97.47	–	52.12	47.88

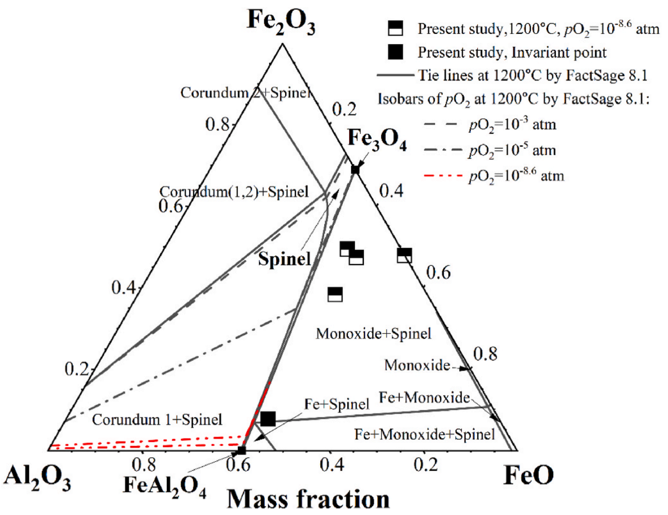

Fig. 11. A comparison of the spinel composition of the present study and the predictions by FactSage 8.1 in the FeO–Fe_2O_3–Al_2O_3 ternary system.

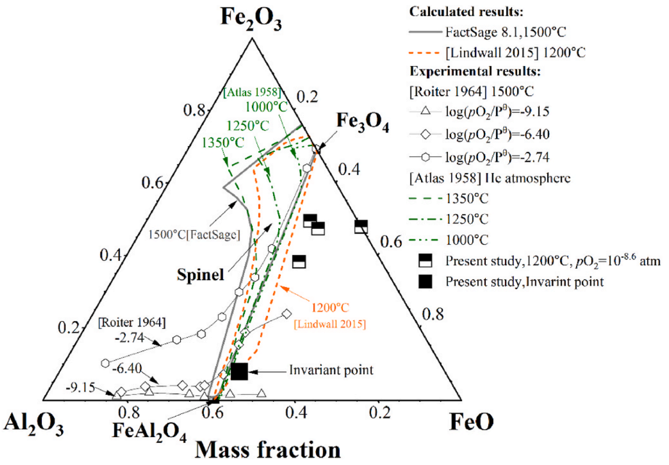

Fig. 12. A comparison of the spinel composition of the present study and the literature [41,43,44] in the FeO–Fe_2O_3–Al_2O_3 ternary system.

FeO–Fe_2O_3–Al_2O_3 system (Fig. 11). The width of the spinel primary phase field was limited by the oxygen partial pressure.

The spinel composition obtained at 1200 °C in this study agreed with the 1200 °C isotherms of the FeO–Fe_2O_3–Al_2O_3 system simulated by Lindwall et al. [41]. With increasing Al_2O_3 concentration in the spinel, the composition point moved toward $FeAl_2O_4$. The Al_2O_3 gave a maximum solubility of approximately 50 wt% in the spinel, which coexisted with the liquid slag and solid tridymite at the invariant point of this study.

4.4. *The fluxing strategy of the FeO_x-SiO_2-Al_2O_3 slag in the smelting of high-alumina copper resources*

The effect of Al_2O_3 concentration on the equilibrium chemical compositions of FeO_x-SiO_2-Al_2O_3 slags under fixed temperature and atmosphere can be quantified based on the present experimental results. As shown in Fig. 9, at 1200 °C and pO_2 of $10^{-8.6}$ atm, Al_2O_3 can dissolve in the liquid phase of FeO_x-SiO_2-Al_2O_3 slags to a maximum concentration of 17 wt%. By varying the Al_2O_3 concentration from 0 to 17 wt%, the Fe/SiO_2 ratio of the liquid phase in the FeO_x-SiO_2-Al_2O_3 slags decreased from 1.2 to 0.6 for the tridymite saturated slags and from 1.8 to 0.6 for the spinel saturated slags, respectively.

The current data can be used to evaluate fluxing strategies for high-Al_2O_3 slags and optimize operations in the secondary copper smelting. As given in Figs. 5 and 9, the Fe/SiO_2 ratios in the slag at the liquidus of the tridymite and spinel primary phase fields decrease with the increasing Al_2O_3 concentration in the slag. Between the two liquidus lines, the slag is fully liquid and no solid phase forms [45]. In industrial practice, when the Al_2O_3 concentration in the raw materials increases, the Fe/SiO_2 ratio in slag needs to be adjusted by adding flux such as silica to obtain a fully liquid slag or a slag with a low solid fraction.

The addition of the fluxes is controlled to avoid over-fluxing based on the isotherms of the FeO_x-SiO_2-Al_2O_3 system. When the slag reaches SiO_2 saturation or spinel saturation, the solid proportion of the slag increases, and the slag tends to be viscous. As a result, the separation kinetics of matte and slag would be affected, and the loss of entrained valuable metals in the slag will increase [46]. For example, at 1200 °C and pO_2 of $10^{-8.6}$ atm, when the Al_2O_3 concentration in slag is 5 wt%, the Fe/SiO_2 ratio in the FeO_x-SiO_2-Al_2O_3 system should be maintained between 1.3 and 1.6 to obtain a fully liquid slag or slag with a low fraction of the solid [42]. Furthermore, when properly controlled, the solids present can help form a protective layer on the refractory lining of the smelting furnace [47]. Therefore, the fluxing strategies for the smelting of high-alumina e-wastes will be regulated based on the current study, to optimize the proportion of solid to limit entertainment while maintaining refractory integrity.

5. Conclusions

The effect of Al_2O_3 on the phase equilibria of fayalite-based slags was investigated under typical oxygen-enriched copper smelting temperature of 1200 °C and pO_2 of $10^{-8.6}$ atm. The equilibrium phase relations of the FeO_x-SiO_2-Al_2O_3 system were experimentally determined for a range of Al_2O_3 concentrations under controlled conditions. Two liquid-solid primary phase fields of liquid-tridymite and liquid-spinel, and one three-phase equilibrium of liquid-tridymite-spinel were observed. The 1200 °C isothermal section of the FeO_x-SiO_2-Al_2O_3 phase diagram at pO_2 of $10^{-8.6}$ atm was constructed based on the present experimental equilibrium phase compositions. The maximum solubility of Al_2O_3 in the liquid oxide of FeO_x–SiO_2-Al_2O_3 slags was determined to be approximately 17 wt% when the liquid slag was saturated with tridymite and spinel.

The current experimental results were compared with the previous data and predictions by MTDATA and FactSage, showing good agreement in the liquid domain. While compared with MTDATA, the spinel phase field in the present results exhibited a lower “FeO” but higher SiO_2 concentration. The spinel phase in equilibrium with liquid slag and tridymite in this study displayed a higher “FeO” but lower Al_2O_3 concentration than the computed data from MTDATA and FactSage. The current results enrich the fundamental data and provide guidance for optimizing fluxing of alumina-rich iron silicate slags and regulating secondary copper smelting operations.

Declaration of competing interest

The authors declare that they have no known competing financial interests or personal relationships that could have appeared to influence the work reported in this paper.

Data availability

The data that has been used is confidential.

Acknowledgements

This work was financed by School of Chemical Engineering, Aalto University. This study utilized the Academy of Finland’s RawMatTERS Finland Infrastructure (RAMI), based jointly at Aalto University, GTK, and VTT in Espoo. Miao Tian and Min Chen are grateful for the financial support from the China Scholarship Council [grant number 202006370337, 201806370217].

Appendix A. Supplementary data

Supplementary data to this article can be found online at https://doi.org/10.1016/j.calphad.2022.102502.

References

[1] V. Forti, C.P. Baldé, R. Kuehr, G. Bel, The Global E-Waste Monitor 2020: Quantities, Flows and the Circular Economy Potential, United Nations University/United Nations of Institute for Training and Research-co-hosted SCYCLE Programme, International Telecommunication Union & International Solid Waste Association, Bonn/Geneva/Rotterdam, 2020.

[2] C. Hagelüken, Recycling of electronic scrap at Umicore’s integrated metals smelter and refinery, World Metall 59 (2006) 152–161.

[3] M. Reuter, C. Hudson, A. van Schaik, K. Heiskanen, C. Meskers, C. Hagelüken, Metal Recycling: Opportunities, Limits, Infrastructure, United Nations Environment Programme, Nairobi, 2013.

[4] A. Muan, Phase equilibrium relationships at liquidus temperatures in the system $FeO-Fe_2O_3-Al_2O_3-SiO_2$, J. Am. Ceram. Soc. 40 (1957) 420–431.

[5] A. Muan, Phase equilibria at liquidus temperatures in the system iron oxide-Al_2O_3-SiO_2 in air atmosphere, J. Am. Ceram. Soc. 40 (1957) 121–133.

[6] B. Zhao, E. Jak, P.C. Hayes, The effect of Al_2O_3 on liquidus temperatures of fayalite slags, Metall. Mater. Trans. B 30 (1999) 597–605.

[7] R.B. Snow, W.J. McCaughey, Equilibrium studies in the system $FeO-Al_2O_3-SiO_2$, J. Am. Ceram. Soc. 25 (1942) 151–160.

[8] M.A.H. Shuva, M.A. Rhamdhani, G.A. Brooks, S. Masood, M.A. Reuter, Thermodynamics data of valuable elements relevant to e-waste processing through primary and secondary copper production: a review, J. Clean. Prod. 131 (2016) 795–809.

[9] R.G. Reddy, C.C. Acholonu, Activity coefficient of $CuO_{0.5}$ in alumina saturated iron silicate slags, Metall. Trans. B 15 (1984) 345–349.

[10] R.G. Reddy, C.C. Acholonu, Distribution of nickel between copper-nickel and alumina saturated iron silicate slags, Metall. Trans. B 15 (1984) 33–37.

[11] M. Nagamori, P.J. Mackey, Distribution equilibria of Sn, Se and Te between $FeO-Fe_2O_3-SiO_2-Al_2O_3-CuO_{0.5}$ slag and metallic copper, Metall. Trans. B 8 (1977) 39–46.

[12] M. Nagamori, P.J. Mackey, P. Tarassoff, Copper solubility in $FeO-Fe_2O_3-SiO_2-Al_2O_3$ slag and distribution equilibria of Pb, Bi, Sb and as between slag and metallic copper, Metall. Trans. B 6 (1975) 295–301.

[13] B. Derin, O. Yücel, The distribution of cobalt between Co-Cu alloys and $Al_2O_3-FeO-Fe_2O_3-SiO_2$ slags: cobalt distribution between alloys and slags, Scand. J. Metall. 31 (2002) 12–19.

[14] L. Klemettinen, K. Avarmaa, P. Taskinen, Slag chemistry of high-alumina iron silicate slags at 1300°C in WEEE smelting, J. Sustain. Metall. 3 (2017) 772–781.

[15] K. Avarmaa, S. Yliaho, P. Taskinen, Recoveries of rare elements Ga, Ge, in and Sn from waste electric and electronic equipment through secondary copper smelting, Waste Manag. 71 (2018) 400–410.

[16] K. Avarmaa, P. Taskinen, The Influence of aluminum on indium and tin behaviour during secondary copper smelting, in: B.R. Davis, M.S. Moats, S. Wang (Eds.), Extr. 2018 Proc. First Glob. Conf. Extr. Metall. Miner. Met. Mater. Ser., Springer International Publishing, Vancouver, Canada, 2018, pp. 1061–1071, https://doi.org/10.1007/978-3-319-95022-8_85.

[17] M. Chen, K. Avarmaa, L. Klemettinen, J. Shi, P. Taskinen, A. Jokilaakso, Experimental study on the phase equilibrium of copper matte and silica-saturated FeO_x-SiO_2-based slags in pyrometallurgical WEEE processing, Metall. Mater. Trans. B 51 (2020) 1552–1563.

[18] M. Chen, K. Avarmaa, L. Klemettinen, J. Shi, P. Taskinen, D. Lindberg, A. Jokilaakso, Equilibrium of copper matte and silica-saturated iron silicate slags at 1300°C and Pso2 of 0.5 atm, Metall. Mater. Trans. B 51 (2020) 2107–2118.

[19] D. Sukhomlinov, L. Klemettinen, H. O’Brien, P. Taskinen, A. Jokilaakso, Behavior of Ga, In, Sn, and Te in copper matte smelting, Metall. Mater. Trans. B 50 (2019) 2723–2732.

[20] A. Fallah-Mehrjardi, T. Hidayat, P.C. Hayes, E. Jak, The effect of Al2O3 on fayalite-based copper smelting slags in equilibrium with matte and tridymite at 1200°C and P(SO2) = 0.25 atm, Int. J. Mater. Res. 111 (2020) 283–289.

[21] H. Abdeyazdan, A. Fallah-Mehrjardi, T. Hidayat, M. Shevchenko, P.C. Hayes, E. Jak, Experimental study of gas-slag-matte-tridymite equilibria in the Cu-Fe-O-S-Si-Al System at 1573 K (1300°C) and P(SO2) = 0.25 atm, J. Phase Equilibria Diffus. 41 (2020) 66–78.

[22] M. Chen, K. Avarmaa, P. Taskinen, R. Michallik, A. Jokilaakso, Investigation on the matte/slag/spinel/gas equilibria in the Cu-Fe-O-S-SiO2-(CaO, Al2O3) system at 1250°C and pSO2 of 0.25 atm, Miner. Process. Extr. Metall. Rev. (2022) 1–12, https://doi.org/10.1080/08827508.2022.2047966.

[23] G.R.F. Alvear Flores, S. Nikolic, P.J. Mackey, Isasmelt^{TM} for the recycling of e-scrap and copper in the U.S. case study example of a new compact recycling plant, JOM 66 (2014) 823–832.

[24] M. Chen, Y. Sun, E. Balladares, C. Pizarro, B. Zhao, Experimental studies of liquid/spinel/matte/gas equilibria in the Si-Fe-O-Cu-S system at controlled $P(SO_2)$ 0.3 and 0.6 atm, Calphad 66 (2019), 101642.

[25] S. Sineva, A. Fallah-Mehrjardi, T. Hidayat, P.C. Hayes, E. Jak, Experimental study of the individual effects of Al2O3, CaO and MgO on gas/slag/matte/spinel equilibria in Cu-Fe-O-S-Si-Al-Ca-Mg system at 1473K (1200°C) and P(SO2) = 0.25 atm, J. Phase Equilibria Diffus. 41 (2020) 859–869.

[26] R. Shimpo, S. Goto, O. Ogawa, I. Asakura, A study on the equilibrium between copper matte and slag, Can. Metall. Q. 25 (1986) 113–121.

[27] X. Wan, J. Shi, L. Klemettinen, M. Chen, P. Taskinen, A. Jokilaakso, Equilibrium phase relations of CaO-SiO2-TiO2 system at 1400°C and oxygen partial pressure of 10-10 atm, J. Alloys Compd. 847 (2020), 156472.

[28] G.F. Bastin, J.M. Dijkstra, H.J.M. Heijligers, PROZA96: an improved matrix correction program for electron probe microanalysis, based on a double Gaussian φ(ρz) approach, X Ray Spectrom. 27 (1998) 3–10.

[29] J. Pouchou, F. Pichoir, Basic expression of “PAP” computation for quantitative EPMA, Proc. ICXOM. 11 (1987) 249–253.

[30] M. Chen, K. Avarmaa, P. Taskinen, L. Klemettinen, R. Michallik, H. O’Brien, A. Jokilaakso, Handling trace elements in WEEE recycling through copper smelting-an experimental and thermodynamic study, Miner. Eng. 173 (2021), 107189, https://doi.org/10.1016/j.mineng.2021.107189.

[31] C.W. Bale, E. Bélisle, P. Chartrand, S.A. Decterov, G. Eriksson, A.E. Gheribi, K. Hack, I.-H. Jung, Y.-B. Kang, J. Melançon, A.D. Pelton, S. Petersen, C. Robelin, J. Sangster, P. Spencer, M.-A. Van Ende, FactSage thermochemical software and databases, 2010–2016, Calphad 54 (2016) 35–53.

[32] J. Gisby, P. Taskinen, J. Pihlasalo, Z. Li, M. Tyrer, J. Pearce, K. Avarmaa, P. Björklund, H. Davies, M. Korpi, S. Martin, L. Pesonen, J. Robinson, Mtdata and the prediction of phase equilibria in oxide systems: 30 years of industrial collaboration, Metall. Mater. Trans. B 48 (2017) 91–98.

[33] D.R. Gaskell, Introduction to the Thermodynamics of Materials, fifth ed., Taylor & Francis, New York, 2008.

[34] D. Shishin, T. Hidayat, A. Fallah-Mehrjardi, P.C. Hayes, S.A. Decterov, E. Jak, Integrated experimental and thermodynamic modeling study of the effects of Al2O3, CaO, and MgO on slag–matte equilibria in the Cu-Fe-O-S-Si-(Al, Ca, Mg) system, J. Phase Equilibria Diffus. 40 (2019) 445–461.

[35] D.J. Duval, S.H. Risbud, J.F. Shackelford, Mullite, in: J.F. Shackelford, R. H. Doremus (Eds.), Ceram. Glass Mater., Springer US, Boston, MA, 2008, pp. 27–39.

[36] M.-L. Bouchetou, J.-P. Ildefonse, J. Poirier, P. Daniellou, Mullite grown from fired andalusite grains: the role of impurities and of the high temperature liquid phase on the kinetics of mullitization and consequences on thermal shocks resistance, Ceram. Int. 31 (2005) 999–1005.

[37] L. Klemettinen, Iron activity measurements and spinel-slag equilibria in alumina-bearing iron silicate slags, J. Alloys Compd. 855 (2021), 157539.

[38] A. Muan, C.L. Gee, Phase equilibrium studies in the system iron oxide-Al_2O_3in air and at 1 atm. O_2 pressure, J. Am. Ceram. Soc. 37 (1956) 207–214.

[39] M. Kudo, E. Jak, P. Hayes, K. Yamaguchi, Y. Takeda, Lead solubility in FeO_x-CaO-SiO_2 slags at iron saturation, Metall. Mater. Trans. B 31 (2000) 15–24.

[40] D. Shishin, V. Prostakova, E. Jak, S.A. Decterov, Critical assessment and thermodynamic modeling of the Al-Fe-O system, Metall. Mater. Trans. B 47 (2016) 397–424.

[41] G. Lindwall, X. Liu, A. Ross, H. Fang, B. Zhou, Z. Liu, Thermodynamic modeling of the aluminum-iron-oxygen system, Calphad 51 (2015) 178–192.

[42] T. Hidayat, A. Fallah-Mehrjardi, P.C. Hayes, E. Jak, Experimental investigation of gas/slag/matte/spinel equilibria in the Cu-Fe-O-S-Si system at 1473K (1200°C) and P(SO2) = 0.25 atm, Metall. Mater. Trans. B 49 (2018) 1750–1765.

[43] L.M. Atlas, W.K. Sumida, Solidus, subsolidus, and subdissociation phase equilibria in the system Fe-Al-O, J. Am. Ceram. Soc. 41 (1958) 150–160.

[44] B.D. Roiter, Phase equilibria in the spinel region of the system FeO-Fe_2O_3-Al_2O_3, J. Am. Ceram. Soc. 47 (1964) 509–511.

[45] N. Cardona, P.J. Mackey, P. Coursol, R. Parada, R. Parra, Optimizing Peirce-Smith converters using thermodynamic modeling and plant sampling, JOM 64 (2012) 546–550.

[46] P. Tan, Applications of thermodynamic modeling in copper converting operations, Int. J. Mater. Res. 98 (2007) 995–1003.

[47] P. Taskinen, M. Kaskiala, P. Hietanen, K. Miettinen, A. Forsström, Microstructure and formation kinetics of a freeze lining in an industrial copper FSF slag, Miner. Process. Extr. Metall. (IMM Trans. Sect. C) 120 (2011) 147–155.